

Investigating (Anti)Neutrino-Carbon Interactions with GENIE Simulations

For the UROP2100 Research Project
Investigation of CP Violation in Neutrino Oscillations
Supervised by Prof. Kam-Biu Luk

XU, Sihong

Department of Physics, The Hong Kong University of Science and Technology

August 2, 2023

Abstract

The investigation of neutrino interactions is deemed to be of great significance in the study of CP violation in neutrino experiments. A (anti)neutrino-nucleon interaction can be classified into elastic scattering, quasielastic scattering (QE), inelastic scattering (IE) and deep inelastic scattering (DIS), combined with a neutral-current (NC) or a charged-current (CC) reaction. Based on this point, in this article (anti)electron neutrino-carbon interactions are simulated using GENIE, with beam energies ranging from 0.1 GeV to 0.5 GeV. The focus of this study is on the analysis of the momentum and energy distributions, as well as the multiplicity of the final-state particles, such as the final-state nucleons, nuclei, and leptons. Both similarities and differences are observed in the neutrino and antineutrino reactions, and qualitative explanations of the phenomena are provided.

1 Introduction

Neutrino mixing is an assumption that the neutrino states ν_e , ν_μ and ν_τ do not have definite masses. Instead they are linear combinations of three states ν_1 , ν_2 and ν_3 with definite masses m_1 , m_2 and m_3 . As a result, when time evolves, a neutrino ν_α with a specific flavour (muon, electron or tauon) can later contain the component of another neutrino ν_β with a different flavour, and the intensity of the ν_α beam would accordingly reduced. This phenomenon is called neutrino oscillation[1] and we may consider the neutrino ν_α is converting into ν_β . Similarly, the antineutrino $\bar{\nu}_\alpha$ can also convert into the antineutrino with a different flavour $\bar{\nu}_\beta$. If there is a difference between the conversion rates of the neutrino ν_α and the anti-neutrino $\bar{\nu}_\alpha$, the charged conjugation and parity symmetry violation (CP violation) occurs.

In order to investigate the CP violation in neutrino oscillation, a precise measurement of the neutrinos and antineutrinos at the detector is very necessary, which requires the complete understanding of the interactions of the neutrinos and antineutrinos with

the detector[2]. Hence in this article, we would mainly focus on the interactions of neutrino ν_ℓ ($\ell = e^-, \mu^-$ or τ^-) and antineutrino $\bar{\nu}_\ell$ with carbon $^{12}_6\text{C}$, which has been proven to be a potential candidate for the detector in the neutrino oscillation experiments.

In essence, the interaction of (anti)neutrino with the carbon could be considered as the interaction of (anti)neutrino with the nucleons, i.e. protons and neutrons. When the energy of the (anti)neutrino is low, it could only scatter off the nucleon N . This is called *elastic scattering* and is obviously a neutral-current (NC) reaction:

$$\nu_\ell + N \rightarrow \nu_\ell + N, \quad (1)$$

$$\bar{\nu}_\ell + N \rightarrow \bar{\nu}_\ell + N. \quad (2)$$

As energy increases, the (anti)neutrino would undergo a charged-current (CC) *quasielastic scattering* (QE):

$$\nu_\ell + n \rightarrow \ell^- + p, \quad (3)$$

$$\bar{\nu}_\ell + p \rightarrow \ell^+ + n. \quad (4)$$

The *inelastic scattering* (IE) happens when the energy of (anti)neutrino is even higher, say larger than the threshold production of a single pion[3]. Table 1 summarizes the neutral current and charged current inelastic processes. Note that all these processes should obey the selection rules of weak interactions[1].

Charged current (CC) reactions	Neutral Current (NC) reactions
$\nu_\ell(\bar{\nu}_\ell) + N \rightarrow \ell^-(\ell^+) + N' + \pi$	$\nu_\ell(\bar{\nu}_\ell) + N \rightarrow \nu_\ell(\bar{\nu}_\ell) + N' + \pi$
$\nu_\ell(\bar{\nu}_\ell) + N \rightarrow \ell^-(\ell^+) + N' + n\pi$	$\nu_\ell(\bar{\nu}_\ell) + N \rightarrow \nu_\ell(\bar{\nu}_\ell) + N' + n\pi$
$\nu_\ell(\bar{\nu}_\ell) + N \rightarrow \ell^-(\ell^+) + N' + \eta$	$\nu_\ell(\bar{\nu}_\ell) + N \rightarrow \nu_\ell(\bar{\nu}_\ell) + N' + \eta$
$\nu_\ell(\bar{\nu}_\ell) + N \rightarrow \ell^-(\ell^+) + Y + K$	$\nu_\ell(\bar{\nu}_\ell) + N \rightarrow \nu_\ell(\bar{\nu}_\ell) + Y + K$
$\nu_\ell(\bar{\nu}_\ell) + N \rightarrow \ell^-(\ell^+) + N' + K(\bar{K})$	$\nu_\ell(\bar{\nu}_\ell) + N \rightarrow \nu_\ell(\bar{\nu}_\ell) + N' + K(\bar{K})$

Table 1: Inelastic scattering of the (anti)neutrino[3]. The symbols N, N' represents the nucleons. The symbols Y represents the hyperons Λ, Σ . The symbols K represents the kaons K^+, K^0 . The symbols \bar{K} represents antikaons K^-, \bar{K}^0 .

When the energy of the (anti)neutrino is sufficiently large, the inner structure of the nucleon could be resolved and the (anti)neutrino will scatter off the quarks inside the nucleon. This is called the *deep inelastic scattering* (DIS) of the (anti)neutrino:

$$\nu_\ell(\bar{\nu}_\ell) + N \rightarrow \ell^-(\ell^+) + N' + \text{jets of hadrons}. \quad (5)$$

The preceding discussion has provided an overview of fundamental (anti)neutrino-nucleon interactions. However, for the (anti)neutrino-nucleus interactions, the situation is much more complicated due to the fact that nucleons cannot be treated as individual entities. The nuclear medium effects, like Fermi motion, binding energy, and nucleon correlations, must be taken into account[4]. Nevertheless, the fundamental cases discussed have contributed significantly to our comprehension of (anti)neutrino-nucleon interactions, providing essential references for the simulation of (anti)neutrino-nucleus interactions in the following sections.

2 Simulation

The simulation of (anti)neutrino-nucleus interactions in this article is conducted by GENIE, which is a neutrino event generator based on the Monte Carlo method[5]. In each event, the target $^{12}_6\text{C}$ is stationary in the laboratory frame, as shown in Figure 1. At $t = 0$, a neutrino (or an antineutrino) is produced in the $+z$ -direction with a specific energy and interacts with the target $^{12}_6\text{C}$. Throughout the interaction, GENIE would record all the particles involved, along with their corresponding physical quantities including momentum, energy, mass, mother and daughter particles, etc. The details of (anti)neutrino-nucleus interactions can then be analyzed by directly extracting information from GENIE event records.

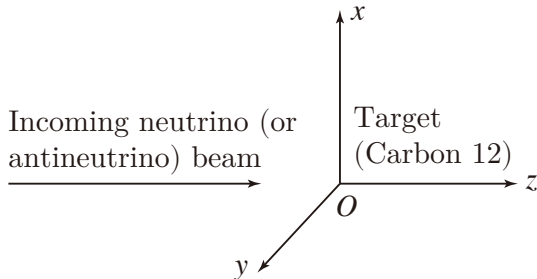


Figure 1: The geometry of the detector in GENIE.

In this article, we primarily focus on electron neutrinos ν_e and their antiparticles $\bar{\nu}_e$, owing to space limitations. The behavior of the other two generations (muon and tauon) is expected to be very similar, given the universality of lepton interactions[1]. The energy of the (anti)neutrino beams is varied over a range of 0.1 to 0.5 GeV¹, enabling an overall observation of elastic scattering, quasi-elastic (QE), inelastic-elastic (IE), and deep inelastic scattering (DIS) reactions. To ensure statistical significance of the results, 20,000 events have been simulated for a specific reaction with the (anti)neutrino beam of a particular energy.

3 Results and Interpretations

During the analysis of the simulation results, our primary focus is on the multiplicity and momentum (or energy) distribution of a specific final-state particle. Multiplicity serves as a crucial indicator that aids in determining the type of interaction, while kinematic parameters (including momentum and energy) are essential for the detection of the final-state particles. Both of these indices are instrumental in providing a more comprehensive understanding of (anti)neutrino-carbon interactions.

As indicated in Figure 1, GENIE will record the 4-momentum (p_x, p_y, p_z and E) of a specific final-state particle. In our analysis, only p_x, p_z and E will be considered since the direction of p_x and p_y are perpendicular to that of the (anti)neutrino beam, and hence the distributions of p_x and p_y are expected to be very similar.

Our analysis will primarily concentrate on the final-state nucleons (protons and neutrons), nuclei (including the final-state ^{12}C) and leptons (including $\nu_e, \bar{\nu}_e, e^+$ and e^-).

¹Note that the natural unit (nu) is used in this article.

3.1 Final-State Nucleons: Protons and Neutrons

Figures 2-13 depict the momentum and energy distributions of a final-state particle as a function of its multiplicity, for (anti)neutrino beams with energies of 0.1 GeV (Figures 2-5), 0.3 GeV (Figures 6-9), and 0.5 GeV (Figures 10-13). The black dots in these figures represent the momentum (or energy) of individual particles, while the red dots correspond to the mean of all values for a specific multiplicity. For Figures 7, 10, 11, and 12, data points in the gray boxes are excluded since the corresponding reactions have been checked to violate the principle of charge conservation and are therefore deemed unphysical in this article.

We begin by examining the common trends observed in the figures. For the distribution of p_x , the mean values for different reactions and multiplicities are found to be close to 0, consistent with the assumption of symmetry in the distribution of components on the xy -plane. In the case of the p_z distribution, for a multiplicity of $n = 1$, the mean values of p_z are positively correlated with the energies of the (anti)neutrino beams, as expected. As the multiplicity n increases, the mean value of p_z gradually decreases towards 0, indicating a convergence towards 0. This trend can be attributed to the fact that with more final-state particles, each particle will acquire less momentum in the $+z$ -direction, which is a reasonable expectation. Finally, for the E distribution, the mean values of p_x and p_z both approach 0 as the multiplicity n increases, leading to a corresponding decrease in the energy E towards the rest mass of the particle, given that

$$E = \sqrt{p^2 + m^2}.$$

With an increase in the energy of the (anti)neutrino beam from 0.1 GeV to 0.5 GeV, the range of momentum (and energy) corresponding to a specific multiplicity is observed to widen. This trend is consistent with the expectation that a higher energy (anti)neutrino beam would increase the probability of final-state particles acquiring larger momentum (and energy) values.

Of note is the observation that the neutrino reaction can produce a maximum of 7 protons and 6 neutrons, while the antineutrino reaction can produce a maximum of 6 protons and 7 neutrons, respectively. This limitation arises from the charged-current quasielastic scattering (CCQE) process. It should be noted that the ^{12}C nucleus consists of 6 protons and 6 neutrons. In the case of the neutrino ν_e , CCQE can convert a neutron to a proton, resulting in 7 protons and 5 neutrons in the final state. Alternatively, if the neutrino ν_e undergoes neutral-current (NC) elastic scattering off the nucleus, and the energy of the neutrino beam is sufficiently high, then 6 protons and 6 neutrons can be knocked out of the nucleus without converting any neutron into a proton. These processes can be written as



As a result, the maximum number of protons and neutrons that can be produced are limited to 7 and 6, respectively. The case for the anti-electron neutrino $\bar{\nu}_e$ is similar:



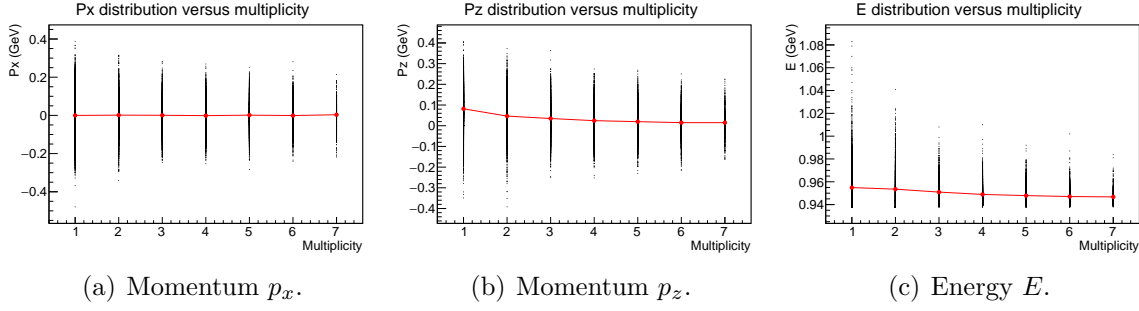


Figure 2: Momentum (energy) distribution versus multiplicity for final-state protons in the reaction $\nu_e + {}^{12}\text{C}$, with $E_\nu = 0.1 \text{ GeV}$.

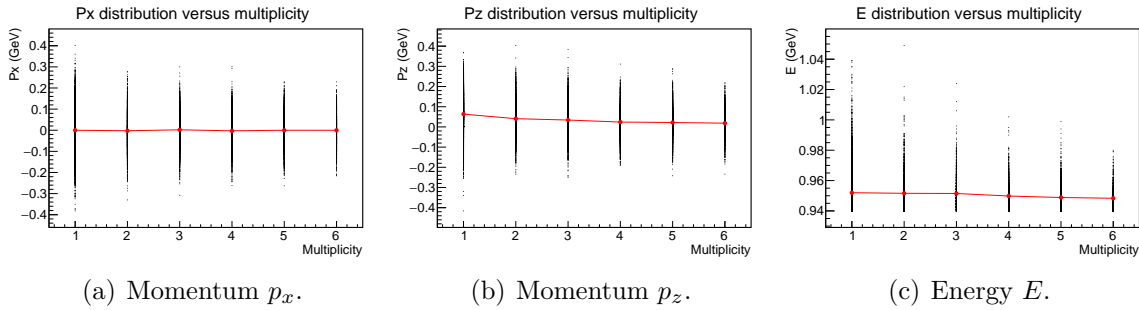


Figure 3: Momentum (energy) distribution versus multiplicity for final-state neutrons in the reaction $\nu_e + {}^{12}\text{C}$, with $E_\nu = 0.1 \text{ GeV}$.

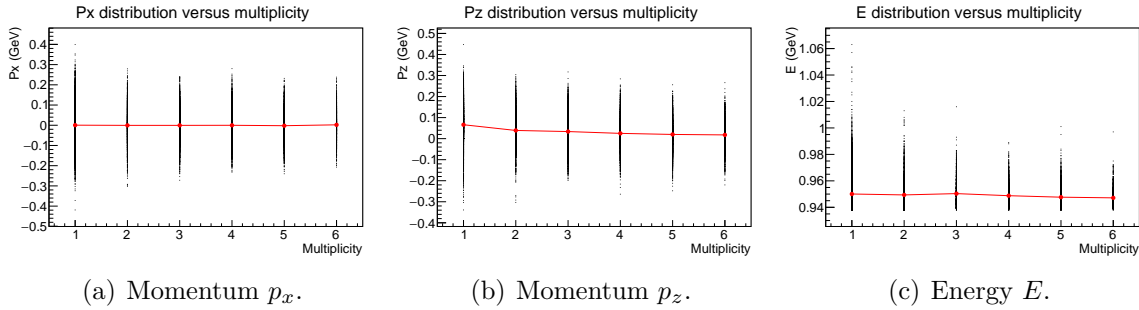


Figure 4: Momentum (energy) distribution versus multiplicity for final-state protons in the reaction $\bar{\nu}_e + {}^{12}\text{C}$, with $E_{\bar{\nu}} = 0.1 \text{ GeV}$.

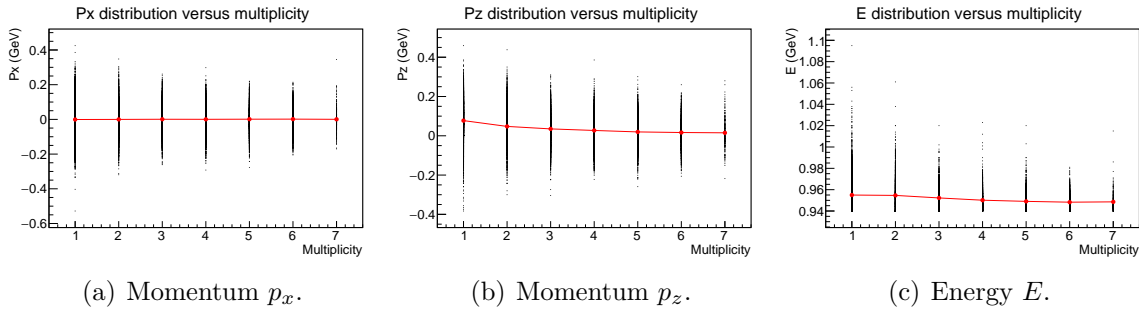


Figure 5: Momentum (energy) distribution versus multiplicity for final-state neutrons in the reaction $\bar{\nu}_e + {}^{12}\text{C}$, with $E_{\bar{\nu}} = 0.1 \text{ GeV}$.

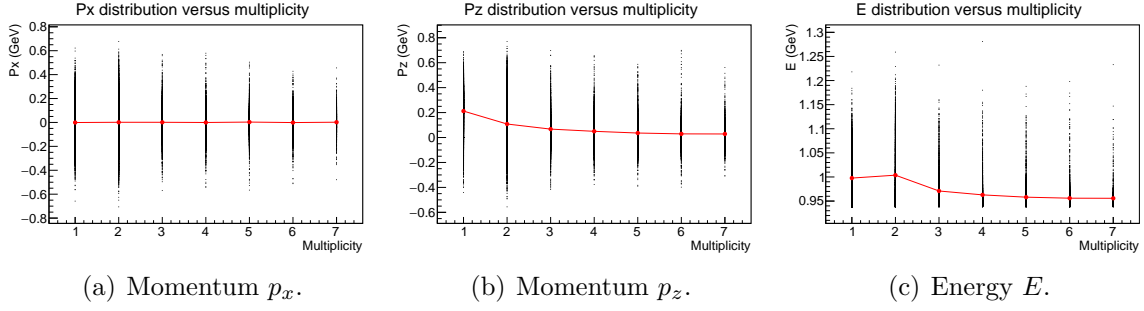


Figure 6: Momentum (energy) distribution versus multiplicity for final-state protons in the reaction $\nu_e + {}^{12}\text{C}$, with $E_\nu = 0.3$ GeV.

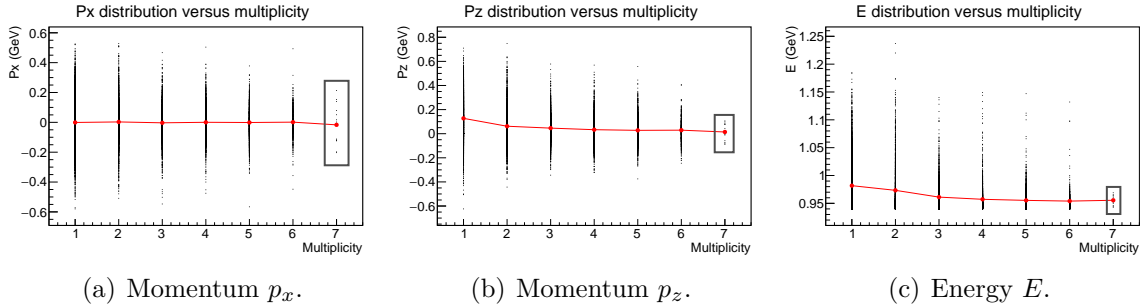


Figure 7: Momentum (energy) distribution versus multiplicity for final-state neutrons in the reaction $\nu_e + {}^{12}\text{C}$, with $E_\nu = 0.3$ GeV.

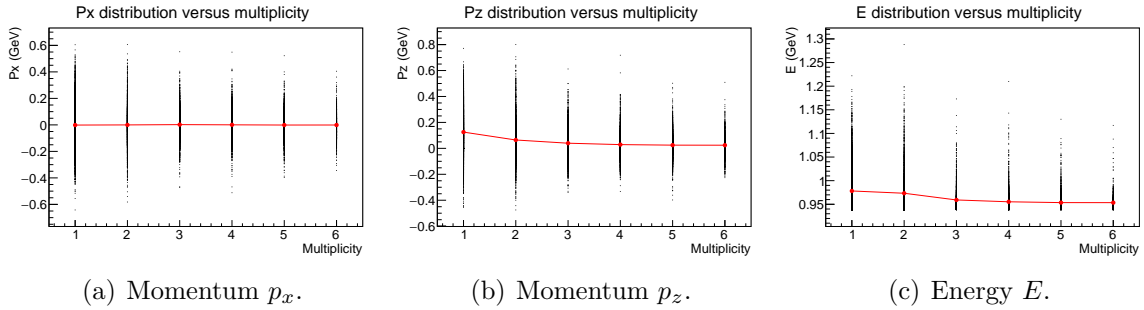


Figure 8: Momentum (energy) distribution versus multiplicity for final-state protons in the reaction $\bar{\nu}_e + {}^{12}\text{C}$, with $E_{\bar{\nu}} = 0.3$ GeV.

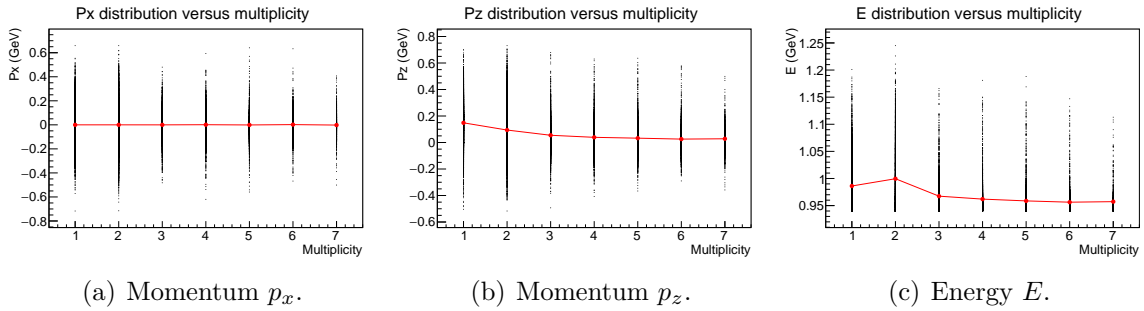


Figure 9: Momentum (energy) distribution versus multiplicity for final-state neutrons in the reaction $\bar{\nu}_e + {}^{12}\text{C}$, with $E_{\bar{\nu}} = 0.3$ GeV.

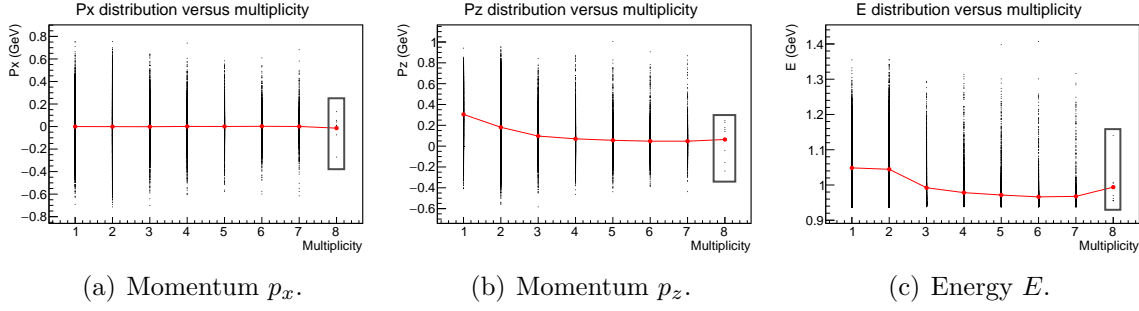


Figure 10: Momentum (energy) distribution versus multiplicity for final-state protons in the reaction $\nu_e + {}^{12}\text{C}$, with $E_\nu = 0.5 \text{ GeV}$.

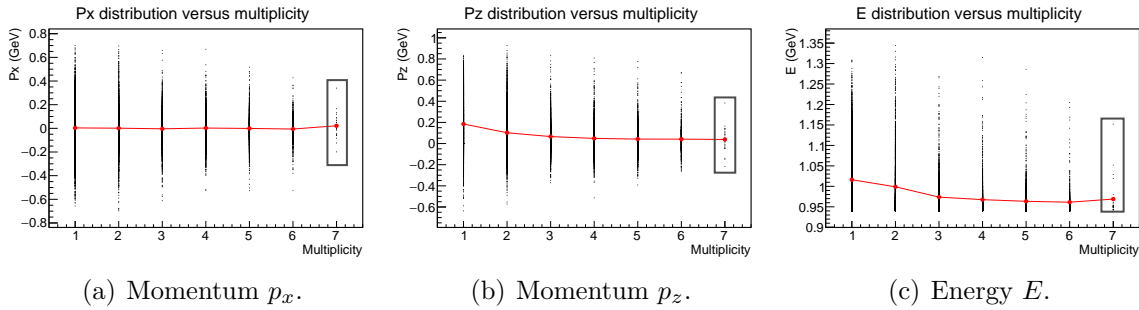


Figure 11: Momentum (energy) distribution versus multiplicity for final-state neutrons in the reaction $\nu_e + {}^{12}\text{C}$, with $E_\nu = 0.5 \text{ GeV}$.

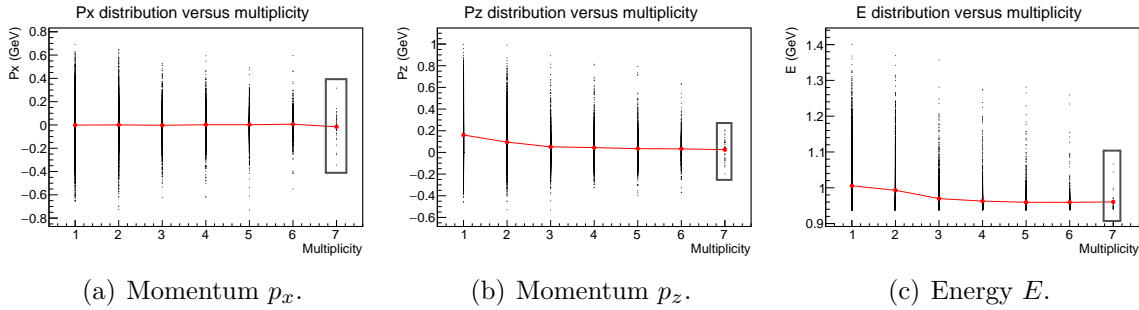


Figure 12: Momentum (energy) distribution versus multiplicity for final-state protons in the reaction $\bar{\nu}_e + {}^{12}\text{C}$, with $E_{\bar{\nu}} = 0.5 \text{ GeV}$.

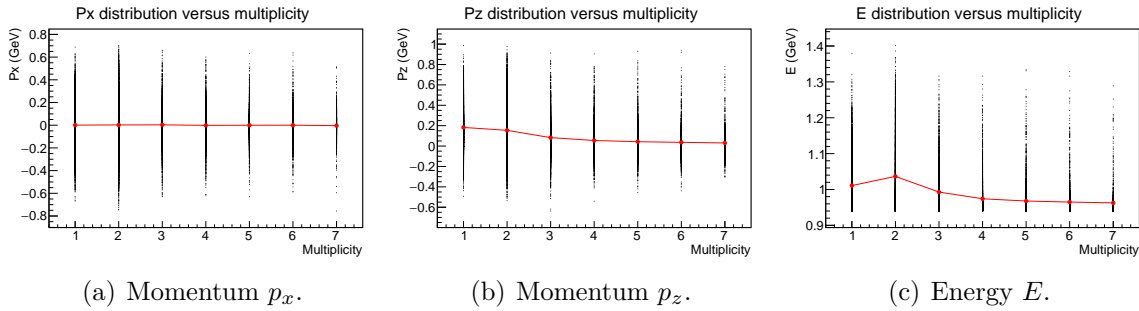


Figure 13: Momentum (energy) distribution versus multiplicity for final-state neutrons in the reaction $\bar{\nu}_e + {}^{12}\text{C}$, with $E_{\bar{\nu}} = 0.5 \text{ GeV}$.

3.2 Final-State Nuclei

We now shift our focus to the final-state nuclei, with the final-state ^{12}C taken into account. Figure 14 illustrates the momentum and energy distributions for neutrino reactions with beam energies of 0.1 GeV, 0.3 GeV, and 0.5 GeV, while Figure 15 depicts the same for antineutrino reactions.

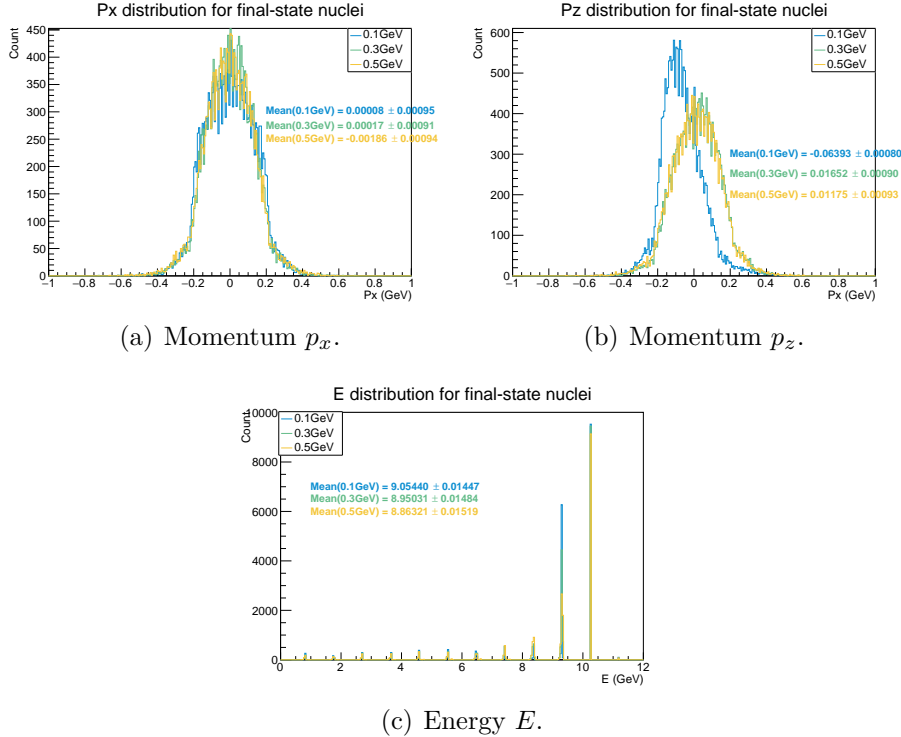


Figure 14: Momentum (energy) distribution for the final-state nuclei in the reaction $\nu_e + ^{12}\text{C}$, with $E_\nu = 0.1$ GeV, 0.3 GeV and 0.5 GeV respectively.

Firstly we examine the commonalities between the neutrino and antineutrino cases. In the p_x distribution, the mean values are consistently close to 0, regardless of the (anti)neutrino beam energy. This is similar to the p_x distribution observed for nucleons. With increasing beam energy, the peaks of the p_x distribution become slightly sharper, indicating that more final-state nuclei have smaller momentum components in the xy -plane. In the case of the p_z distribution, for low beam energies, the mean value of p_z is negative. This can be attributed to the relatively large p_z momentum of the knocked-out nucleons from the carbon nucleus. As the beam energy increases, the mean values of p_z converge towards 0, similar to the final-state nucleons. As for the E distributions, they are not continuous, as the momenta of the final-state nuclei are much smaller than their rest masses. Additionally, there are significantly more final-state nuclei with large E values compared to smaller E values, as the probability of knocking out all nucleons in the ^{12}C nucleus is quite low. Furthermore, as the beam energy increases, there are fewer final-state nuclei with large E values, since the higher energy beam has a greater probability of knocking out more nucleons from the ^{12}C nucleus.

It is worth noting that the momentum and energy distributions for neutrino and antineutrino reactions exhibit significant similarity. One possible explanation for this

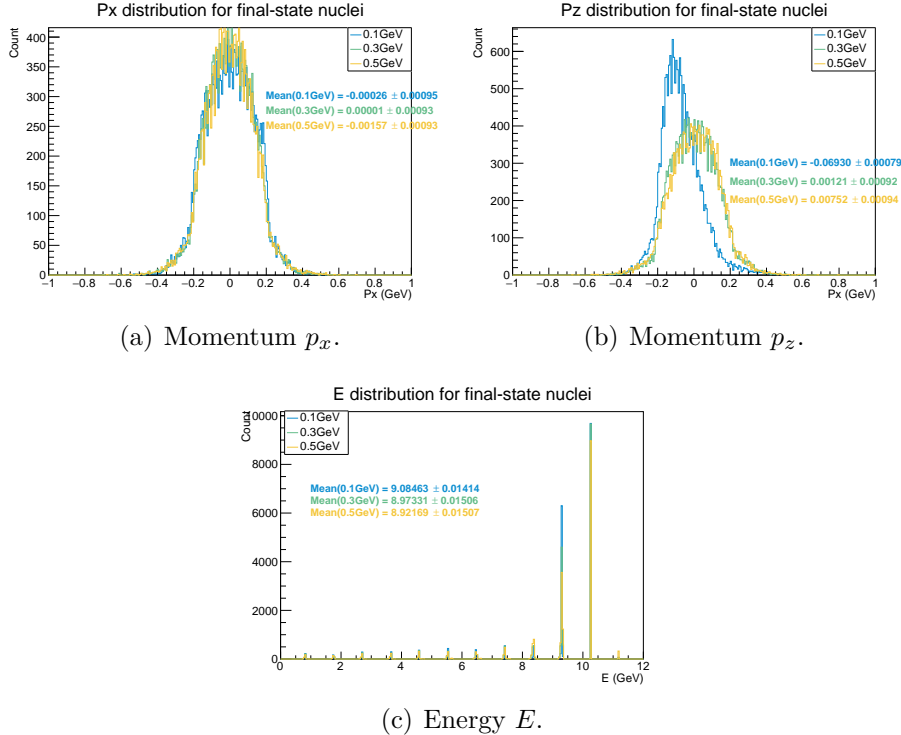


Figure 15: Momentum (energy) distribution for the final-state nuclei in the reaction $\bar{\nu}_e + {}^{12}\text{C}$, with $E_{\bar{\nu}} = 0.1 \text{ GeV}, 0.3 \text{ GeV}$ and 0.5 GeV respectively.

observation is that the final-state nuclei are produced in a similar pattern for both neutrino and antineutrino reactions.

3.3 Final-State Leptons

In this section, we direct our attention to the examination of the final-state leptons, with their corresponding histograms presented in Figures 16-19. It has been established in previous sections that the p_x distribution for final-state particles is symmetric about 0, and thus the patterns of the final-state leptons are expected to be similar. Hence, in this section, we focus exclusively on the p_z and E distributions.

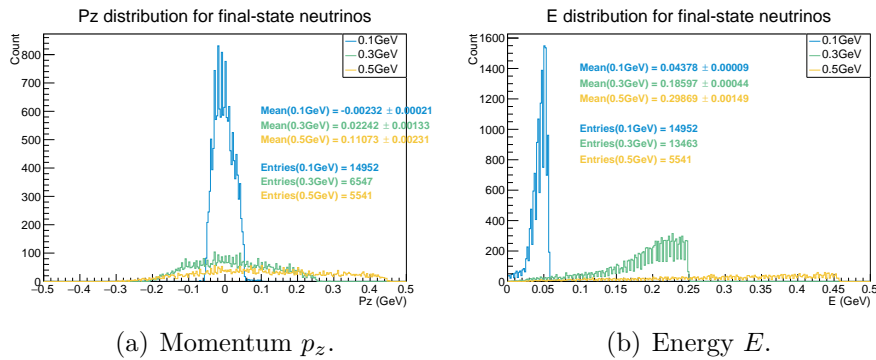


Figure 16: Momentum (energy) distribution for the final-state neutrinos ν_e in the reaction $\nu_e + {}^{12}\text{C}$, with $E_{\nu} = 0.1 \text{ GeV}, 0.3 \text{ GeV}$ and 0.5 GeV respectively.

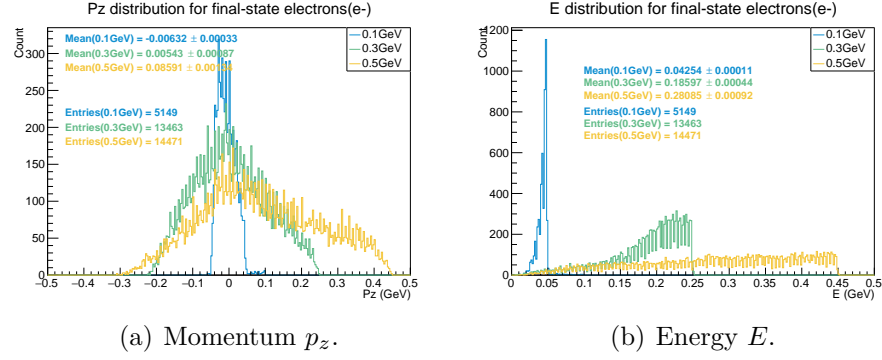


Figure 17: Momentum (energy) distribution for the final-state electrons e^- in the reaction $\nu_e + {}^{12}\text{C}$, with $E_\nu = 0.1$ GeV, 0.3 GeV and 0.5 GeV respectively.

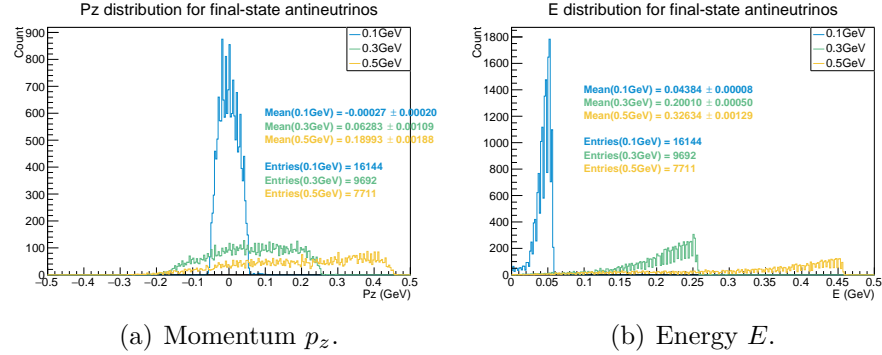


Figure 18: Momentum (energy) distribution for the final-state antineutrino $\bar{\nu}_e$ in the reaction $\bar{\nu}_e + {}^{12}\text{C}$, with $E_{\bar{\nu}} = 0.1$ GeV, 0.3 GeV and 0.5 GeV respectively.

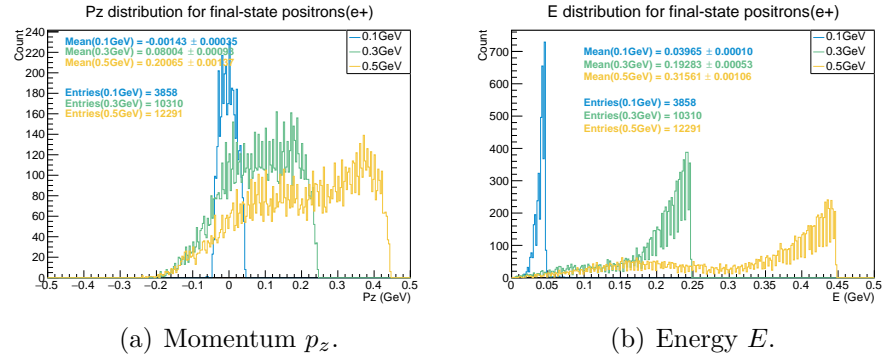


Figure 19: Momentum (energy) distribution for the final-state positrons e^+ in the reaction $\bar{\nu}_e + {}^{12}\text{C}$, with $E_{\bar{\nu}} = 0.1$ GeV, 0.3 GeV and 0.5 GeV respectively.

Turning to the neutrino case, it should be noted that the presence of final-state neutrinos indicates a neutral-current (NC) reaction. As depicted in Figure 16(a), the momentum distribution of final-state neutrinos exhibits a peaked structure. At a beam energy of 0.1 GeV, the peak is sharp, while at higher beam energies, the peak broadens significantly, with an increase in the mean value. This behavior can be attributed to

the fact that the neutrinos can acquire a larger momentum p_z on average as the beam energy increases. With regard to the energy E of final-state neutrinos, the number of neutrinos with energy E increases as E increases, until E approaches the beam energy E_ν . This observation implies that the neutrino has a greater probability of losing less energy in the reaction. Moreover, the number of final-state neutrinos decreases as the beam energy increases, indicating a decrease in the probability of NC reaction with increasing beam energy.

Concerning the final-state electrons, as depicted in Figure 17, the results are consistent with the aforementioned observations. The number of final-state electrons increases with increasing beam energy, indicating an increase in the number of charged-current (CC) reactions. Additionally, both Figure 17(a) and (b) exhibit significant similarity to Figure 16(a) and (b), respectively. The reason might be that the final-state electron shares a vertex with the initial-state neutrino in a CC reaction, just like the final-state neutrino shares a vertex with the initial-state neutrino in a NC reaction.

Regarding Figures 18 and 19, it is evident that despite some differences like mean values and maximum, the momentum and energy distributions of final-state antineutrinos and positrons exhibit similar patterns to those of their respective antiparticles.

4 Conclusions

We now arrive at a conclusion based on the results presented in the previous sections.

- For the final-state nucleons, the momentum and energy distributions in neutrino and antineutrino reactions is quite similar. The main difference is that the multiplicity of protons and neutrons in neutrino reactions is at most 7 and 6 respectively, whereas in antineutrino reactions, the multiplicity of protons and neutrons is at most 6 and 7 respectively.
- For the final-state nuclei, similar patterns are observed in both the neutrino and antineutrino reactions.
- For the final-state leptons, neutrino reactions and antineutrino reactions produce different groups of leptons. The neutrino reactions can produce ν_e or e^- in final state and the antineutrino can produce $\bar{\nu}_e$ or e^+ in final state. However, the patterns of final-state neutrinos and electrons in neutrino reactions resemble those of their corresponding antiparticles in antineutrino reactions.
- As the beam energy increases from 0.1 GeV to 0.5 GeV, the number of CC reactions increases while the number of NC reactions decreases for both the neutrino and antineutrino reactions. Also, the probability of having an elastic scattering decreases while the probabilities for having a QE, IE or DIS reaction increase, for both the neutrino and antineutrino reactions.

In summary, the momentum and energy distributions of certain final-state particles display a degree of similarity. Nevertheless, discernible differences are also evident, particularly in the case of final-state nucleons and leptons.

5 Outlook

In this article, (anti)neutrino-carbon interactions are simulated using GENIE. However, it should be noted that the results obtained from simulations may differ from reality. The Monte Carlo method used by GENIE has inherent limitations in its ability to fully capture the complexity of the interactions. Furthermore, our understanding of the GENIE event records remains incomplete, with some event records presenting reactions that are not conserved in our understanding, and hence have been excluded from this study. Additionally, quantities of pseudo particles in the event records remain challenging to interpret accurately in the reaction.

The focus of our work is on summarizing the momentum and energy distribution of several final-state particles based on simulation results. Future research may concentrate on other physical quantities, such as cross-section, and other final-state particles, such as hyperons and kaons. Moreover, a comprehensive understanding of (anti)neutrino-nucleus interactions could be gained by studying the differences between (anti-)muon neutrino-carbon and (anti-)electron neutrino-carbon interactions.

Additional Information

The programs of extracting the information from GENIE are not shown here due to the space limitations. Readers who are interested may refer to here.

Acknowledgements

I would like to express my sincere gratitude to Prof. Kam-Biu Luk for his invaluable guidance, support and supervision throughout this research project. Prof. Luk not only imparted his extensive knowledge of particle physics, but also provided us with invaluable suggestions on how to conduct researches in a rigorous and systematic manner. Thanks to Prof. Luk, I have gained a wealth of knowledge through this project.

References

- [1] B. R. Martin and G. Shaw. *Particle physics*. Wiley Blackwell, 2017.
- [2] K.S. McFarland. Neutrino interactions. *Nuclear Physics B - Proceedings Supplements*, 235–236:143–148, 2013. doi: 10.1016/j.nuclphysbps.2013.04.004.
- [3] M. Sajjad Athar and S. K. Singh. *The physics of Neutrino Interactions*. Cambridge University Press, 2020.
- [4] H. Haider, F. Zaidi, M. Sajjad Athar, S.K. Singh, and I. Ruiz Simo. Nuclear medium effects in structure functions of nucleon at moderate Q^2 . *Nuclear Physics A*, 943: 58–82, 2015. doi: 10.1016/j.nuclphysa.2015.08.008.
- [5] C. Andreopoulos et al. The GENIE Neutrino Monte Carlo Generator. *Nucl. Instrum. Meth. A*, 614:87–104, 2010. doi: 10.1016/j.nima.2009.12.009.